TECHNICAL REPORT ARAED-TR-87027

PERFORMANCE CHARACTERISTICS OF MAGNESIUM-SODIUM NITRATE FLARES IN OXYGEN-NITROGEN ATMOSPHERES

PATRICIA L FARNELL
FRANCIS R. TAYLOR

OCTOBER 1987

US ARMY
ARMAMENT MUNITIONS
& CHEMICAL COMMAND
ARMAMENT RDE CENTER

U. S. ARMY ARMAMENT RESEARCH, DEVELOPMENT AND ENGINEERING CENTER
ARMAMENT ENGINEERING DIRECTORATE
PICATINNY ARSENAL, NEW JERSEY

UNCLASSIFIED

SECURITY CLASSIFICATION OF THIS PAGE (When Data Entered)

REPORT DOCUMENTATION PAGE

READ INSTRUCTIONS BEFORE COMPLETING FORM

1. REPORT NUMBER Technical Report ARAED-TR-87027	2. GOVT ACCESSION NO. AD-A185 274	3. RECIPIENT'S CATALOG NUMBER
4. TITLE (and Subtitle) Performance Characteristics of Magnesium-Sodium Nitrate Flares in Oxygen-Nitrogen Atmospheres		5. TYPE OF REPORT & PERIOD COVERED 6. PERFORMING ORG. REPORT NUMBER
7. AUTHOR(s) Patricia L. Farnell Francis R. Taylor		8. CONTRACT OR GRANT NUMBER(s)
9. PERFORMING ORGANIZATION NAME AND ADDRESS ARDEC, AED Energetics and Warheads Div (SMCAR-AEE-P) Picatinny Arsenal, NJ 07806-5000		10. PROGRAM ELEMENT, PROJECT, TASK AREA & WORK UNIT NUMBERS
11. CONTROLLING OFFICE NAME AND ADDRESS ARDEC, IMD STINFO Br (SMCAR-IMI-I) Picatinny Arsenal, NJ 07806-5000		12. REPORT DATE October 1987 13. NUMBER OF PAGES 28
14. MONITORING AGENCY NAME & ADDRESS(if different from Controlling Office)		15. SECURITY CLASS. (of this report) 15a. DECLASSIFICATION/DOWNGRADING SCHEDULE

16. DISTRIBUTION STATEMENT (of this Report)

Approved for public release; distribution is unlimited.

17. DISTRIBUTION STATEMENT (of the abstract entered in Block 20, if different from Report)

18. SUPPLEMENTARY NOTES

19. KEY WORDS (Continue on reverse side if necessary and identify by block number)

Magnesium-sodium nitrate flares
Pyrotechnic compositions
Atmospheric compositions
Burning rates
Luminous output
Luminous efficiency
Pyrotechnic flares

20. ABSTRACT (Continue on reverse side if necessary and identify by block number)

The burning rates and light outputs produced by miniature flares containing magnesium and sodium nitrate have been studied as a function of metal-oxidant ratio and oxygen content of the atmosphere. Also studied were the effects of loading pressure and the use of an organic binder upon the combustion process. In these studies, various atmospheres containing nitrogen and oxygen were used. It was found that the burning rates of the flares were unaffected by the oxygen content of the atmosphere, indicating that radiation feedback from the flame has only a minor influence on the burning rate. It was also (cont)

DD FORM 1 JAN 73 1473 EDITION OF 1 NOV 65 IS OBSOLETE

UNCLASSIFIED

SECURITY CLASSIFICATION OF THIS PAGE (When Data Entered)

A

20. ABSTRACT (cont)

found that increasing the loading pressure caused only minor changes in the burning rates of the system indicating that the burning process is not greatly influenced by the reduced gaseous permeability caused by increased loading pressure. However, the burning rate appears to be controlled by exothermic processes occurring at or very near to the burning surface.

For all systems, the burning compositions produced very low light outputs when oxygen was excluded from the atmosphere. With increasing oxygen content, the light output was increased by a large factor. Furthermore, increasing the total gaseous pressure (systems containing 20% and 100% oxygen)also caused an increase in light output. It appears that the majority of the light is produced by combustion of the metal in the air, and that the reaction is limited by diffusion of oxygen into the flame zone from the surrounding atmosphere. Gases produced by the decomposition of a binder can have an effervescent effect, producing smaller metal droplets which are more easily consumed. Consequently, binder systems produced the highest outputs of all the systems investigated.

CONTENTS

TABLES

FIGURES

INTRODUCTION

The luminosity of pyrotechnic flare flames can be produced by a two-stage process. In the first stage, metal particles are melted, partially vaporized and oxidized by the decomposition products of the oxidizer at or very near the flame surface. Hot gases produced by this reaction heat the unreacted metal particles and eject them into the atmosphere. The second stage process then consists of the combustion of these metal particles with atmospheric oxygen, and with the gases produced by the decomposition of the oxidizer.

It is the objective of the study to investigate the second stage process, that is, the luminosity that occurs because of the atmospheric combustion of the metal particles produced by burning Mg-$NaNO_3$ compositions. The extensive investigations of single particle combustion (refs 1 through 3) have been of considerable help in understanding processes occurring in the present study.

EXPERIMENTAL PROCEDURE

Samples consisted of 300 to 400 mg of the composition capped with 100 mg of a nonilluminating igniter composition. The compositions were pressed in a 6.4-mm die at pressures of either 10 or 33 kpsi.* This procedure produced pellets which were about 0.64 cm long. Samples were then wrapped with two layers of Kraft paper tape to form a case which prevents side burning.

The pellets were placed in the center of an upright cylindrical chamber 25 cm in diameter by 23 cm in height with a total volume of 11.5 liters. There was a removable quartz window in the center of the wall for observing the burning pellet. The chamber was evacuated, then filled

---

* kpsi equals pounds per square inch in thousands.

with the proper gas mixture to a total pressure of 760 Torr. The pellets were ignited by a hot wire, and the light intensity produced by the burning composition was measured by a calibrated RCA 926 vacuum phototube located 85 cm in front of the window. The phototube had corrective filters to give response essentially equivalent to that of the human eye. The voltage developed by the phototube current flowing through a standard resistor was recorded by a fast-response oscillograph. The duration of burning was reported in seconds, the burning rate (BR) in cm/min, the average luminous output (LO) in candles/in.^{2} of flare surface area, the luminous efficiency (LE) in candle-sec/g of composition, and the adjusted LE in candle-sec/g of magnesium (Mg),

At least six pellets were burned in each atmosphere. Where results for a pellet were very far from the average in at least two of the three measured parameters, the values were discarded and several more pellets were burned. The average deviation for each average value was ± 10 to 15%, and all points were within 1.96 standard deviation.

The amount of Mg remaining unburned from the flares was determined by burning the pellets in a Paar bomb, adding water to react with any sodium formed, then adding H_2SO_4 to the residue and measuring the amount of H_2 evolved (ref 4).

RESULTS AND DISCUSSION

Compositions of Mg-$NaNO_3$ pressed at 10 kpsi and mixed in proportions of 60-40, 50-50, and 40-60 weight percentages were burned in N_2-O_2 atmospheres of 0, 20, 40, 60, 80, and 100 volume percent of O_2 at different pressures. The effect of loading pressure was investigated by burning the 50% Mg composition pressed at 10 and 33 kpsi. A composition of 47% Mg/47% $NaNO_3$/6% Laminac was studied to determine the effect of binder on the composition.

Effect of Mg Content on Performance Characteristics

The values for the burning rates of the binary compositions pressed at 10 kpsi are listed in table 1. The BR generally increases as the amount of Mg in the composition is increased. For 50

and 40% Mg, the BR is almost constant over the range of atmospheres indicating that there is little radiation feedback from the flame zone to the composition.

Table 1. Average burning rates of 60-40, 50-50, 40-60 Mg-$NaNO_3$ compositions in N_2-O_2 atmospheres

	60% Mg		50% Mg		40% Mg	
Volume % O_2	BR (cm/min)	RSD*	BR (cm/min)	RSD*	BR (cm/min)	RSD*
0	35.1	0.172	20.4	0.072	15.5	0.112
20	27.4	0.080	19.6	0.065	15.3	0.121
40	25.2	0.126	19.0	0.068	15.6	0.156
60	21.2	0.129	19.3	0.109	15.5	0.140
80	20.0	0.113	18.8	0.066	14.8	0.083
100	20.2	0.059	20.0	0.091	13.5	0.056

* RSD = relative standard deviation = standard deviation/average value

For the composition containing 60% Mg, there is an apparent decrease in BR as the O_2 content of the atmosphere is increased. Repeated duplication of this result confirmed that it is real and could result from the oxygen supply in the vicinity of the surface being depleted, therefore, allowing melted magnesium to flow from the reaction zone without reacting.

The LO for these compositions increased with increasing oxygen content of the atmosphere (fig. 1). The values of LO in pure nitrogen are very low, and the addition of 20% oxygen causes a large increase in these values. This dependence on atmospheric oxygen of the luminosity of the flame signifies the inefficiency of the sodium nitrate in its reaction with the metal. Since the stoichiometry of Mg-$NaNO_3$ reaction is 45.9% Mg according to the equation

$$6\ Mg + 2\ NaNO_3 \rightarrow 6\ MgO + 2\ Na + N_2$$

the composition containing 40% Mg should be less dependent on atmospheric O_2 than the

metal-rich compositions. While this is true, the addition of O_2 causes a large increase in LO for this composition as it did for the others. After the initial increase, the LO for all compositions increases linearly with increasing O_2 content of the atmosphere.

As expected, the LO increases in a simulated air atmosphere as the amount of Mg in the composition is increased due to the greater quantity of Mg available to be oxidized (fig.2)

The luminous efficiency, adjusted for the Mg content of the composition, is plotted versus the O_2 content of the atmosphere (fig. 3). These plots show that there was a very large increase in the LE on the addition of O_2 as there was for LO. The efficiencies are almost the same for all Mg contents, indicating a maximum rate of reaction governed by the amount of O_2 in the atmosphere.

Effect of Loading Pressure on Performance Characteristics

The effect of loading pressure on the performance was studied by burning the 50% Mg composition consolidated at 10 and 33 kpsi. The BR was 19.6 cm/min for the composition pressed at 10 kpsi and 14.9 cm/min for that pressed at 33 kspi. However, even though the gaseous permeability changed by a factor of 4 (ref 5), the mass burning rate for these compositions changed minimally, from 0.165 to 0.155 g/sec, respectively. Although the pellet is shorter and denser when loaded at higher pressure, the same weight of material was burned per unit time. This observation is confirmed by comparing the luminous intensities and efficiencies of the two compositions (figs. 4 and 5). The LO's are essentially the same as would be the case if equal weights of composition are being burned in the same time. The LE's for the composition pressed at 33 kpsi are slightly higher than those for the one pressed at 10 kpsi. This is probably because the metal particles are not ejected as freely from the composition consolidated at the higher pressure due to its more compact nature, thereby permitting the particles to burn more completely before passing from the flame zone.

Effect of Binder on Performance Characteristics

To determine the effect of adding a binder to the Mg-$NaNO_3$ binary, a composition was burned which contained 47% Mg/47% $NaNO_3$/6% Laminac. This composition retains the 1:1 ratio of Mg:$NaNO_3$ which exists for the composition containing 50% Mg with which it is compared. The BR was cut in half (from 19.6 to 9.68 cm/min) by adding the binder. This is to be expected since the decomposition of the binder reduces the surface temperature, thereby slowing the reaction rate. This lower reaction rate results in a somewhat lower LO (fig. 6). On the other hand, due to more efficient combustion of the fuel, the LE is greatly increased (fig. 7). The amount of Mg remaining unburned in various compositions points out this more efficient combustion. Ninety-seven percent of the Mg is consumed for the binder composition burned in pure O_2 (table 2); however, large amounts of Mg are left unburned from the binary compositions. There is a correlation between the amount of Mg consumed and the LE produced by the burning compositions (table 2). It appears that the presence of Laminac is very beneficial to the combustion process.

Table 2. Magnesium consumed in magnesium-sodium nitrate flares

Composition by weight percentages	Percent O_2 in atmosphere	Percent Mg consumed	Percent LE/LE_{max}[a]
40 Mg/60 $NaNO_3$	20	25	19
50 Mg/50 $NaNO_3$	20	25	20
40 Mg/60 $NaNO_3$	100	42	50
50 Mg/50 $NaNO_3$	100	44	50
47 Mg/47 $NaNO_3$/6 Laminac[b]	100	97	100

[a] LE_{max} is the LE for 47%/Mg/47% $NaNO_3$/6% Laminac burned in pure O_2.

[b] Laminac is made of 98.5% Laminac 4016 Resin, 1% Lupersol, and 0.5% Nuodex.

Effects of Gaseous Pressure and Consolidation Pressures on Burning Rates of Mg-$NaNO_3$ Flares

Several experiments were conducted to determine the effects of O_2 content, atmospheric pressure, and consolidation pressure on the burning rates of Mg-$NaNO_3$ pellets. In these experiments, gas containing 20 and 100% O_2 was used at pressures of 0.5, 1.0, and 2.0 atmospheres. These results are shown graphically in figure 8 using flare pellets consolidated at 10 and 33 kpsi. Although these are only crude graphs based on three points each, they indicate two important trends: (1) the burning rates of the compositions, consolidated at the lower pressure of 10 kpsi and burned in 20% O_2, increase linearly with increasing atmospheric pressure; (2) the pellets consolidated at the higher pressure of 33 kpsi have burning rates which begin to rise exponentially with increasing atmospheric pressure.

Several phenomena begin to occur as the atmospheric pressure increases. The gaseous reaction zone is increasingly confined to the flare surface resulting in greater transfer of energy back to the composition. Also, increasing atmospheric pressure increases the pressure gradient and ensuing permeation into the flare grain.

At the lower consolidation pressure of 10 kpsi, the burning rate increases due to increased permeation with increasing pressure for gases containing both 20 and 100% O_2. However, when the consolidation pressure is increased to 33 kpsi, the transfer of thermal energy into the flare by conductivity is becoming increasingly important. This enhancement in thermal conductivity results from the greater proximity of the highly conductive metal particles due to the increased consolidation pressure. As the O_2 content and atmospheric pressure increase, the reaction rate increases rapidly, pumping greater energy into the flare surface. This results in a rapid increase in burning rate.

CONCLUSIONS

The burning of magnesium-sodium nitrate flares occurs by two processes: condensed phase and vapor phase. In the condensed phase, metal particles are melted, partially vaporized,

and oxidized by the molten oxidizer and/or its decomposition products at or very near the flare surface. In addition, the hot gases produced by these reactions heat the unreacted metal particles and eject them into the atmosphere. In the vapor phase reaction, these ejected metal particles react with atmospheric oxygen and with the gases produced by the decomposition of the oxidizer.

The processes occuring in the condensed phase have been found to be essentially independent of the atmospheric reactions (at least for the compositions containing 40 and 50% Mg), as evidenced by the constant BR's for these compositions with increasing O_2 content of the atmosphere. This study has clearly shown that the luminous output of the gas phase reactions increase very rapidly with increasing O_2 content without the resulting radiation feedback changing the BR. This is because the absorbed radiation is being used to vaporize the surface of the molten condensed phase and not being transferred back into the solid unburned composition. The molten phase is concomitantly being cooled by the vaporization of the liquid Mg and the decomposition of the organic binder.

The predominant light-producing processes occur in the vapor phase as shown by numerous spectroscopic investigations. These processes include the production of excited Na (line broadened) and Planckian greybody radiation from solid MgO, both as free product and coating material. This radiation is highly oxygen dependent as shown by the very low luminous output (LO) and luminous efficient (LE) values obtained when Mg-$NaNO_3$ pellets were burned in pure N_2. As the O_2 content of the atmosphere increases, the LO and LE values increase dramatically. This rapid increase in LO obviously results from a significant increase in reaction temperature as predicted by the Stefan-Boltzman law which states that the total black-body radiant flux/unit area is proportional to the fourth power of the absolute temperature.

The rapid reaction of Mg with atmospheric O_2 causes a partial depletion of O_2 in the flame zone which must be replenished by diffusion from outside the zone. This partial depletion can cause the burning metal particles to become extinguished and pass unburned from the flame zone. This effect was observed in the incomplete burning which occured even with 100% O_2 atmospheres for the 50% Mg/50% $NaNO_3$ composition.

Returning to the condensed phase, several experiments were conducted to determine the effects of O_2 content, atmospheric pressure, and consolidation pressure on burning rate (BR) of Mg-$NaNO_3$ pellets. It was found that at the lower consolidation pressure of 10 kpsi, the BR increased, probably due to increased gaseous permeation from increased pressure with atmospheres containing both 20 and 100% O_2. However, when the consolidation pressure is increased to 33 kpsi, the transfer of thermal energy into the flare by conductivity is becoming increasingly

important. This enhancement in thermal conductivity results from the greater proximity of the highly conductive metal particles due to the the increased consolidation pressure. As the O_2 content and atmospheric pressure increase, the reaction rate increases rapidly, pumping greater energy into the flare surface. This results in a rapid increase in buring rate.

Finally it was discovered that the presence of only 6% of an organic binder had a very significant and desirable effect on increasing combustion efficiency. For example, a 50/50 $Mg/NaNO_3$ composition burning in a 100% O_2 atmosphere used only 44% of the available Mg, while similar mixes containing 6% binder (Laminac) consumed 97% of the Mg. It is postulated that the gases generated by the decomposition of a binder produce metal droplets which are more easily consumed. The binder system resulted in the highest luminous efficiencies of all the systems investigated.

REFERENCES

1. Christensen, H.C., Knipe, R.H., and Gordon, A.S., Pyrodynamics, vol 3, 1965, pp 99-119.

2. Brzustkowski, T.A. and Glassman, I., Hetergeneous Combustion, Academic Press, New York, NY, 1965, p 75, p 117.

3. Cassel, H.M. and Liebman, I., Combustion and Flame, vol 3, 1959, p 467.

4. Hogan, V.D. and Taylor, F.R., Analytical Chemistry, vol 40, 1963, p 1387.

5. Farnell, P.L., Beardell, A.J., and Taylor, F.R., The Effects of Gaseous Atmospheres and Gas Permeability on the Performance of Magnesium Sodium Nitrate Flares, Third Quadripartite Ammunition Conference, Chorley, UK, Sept 1971.

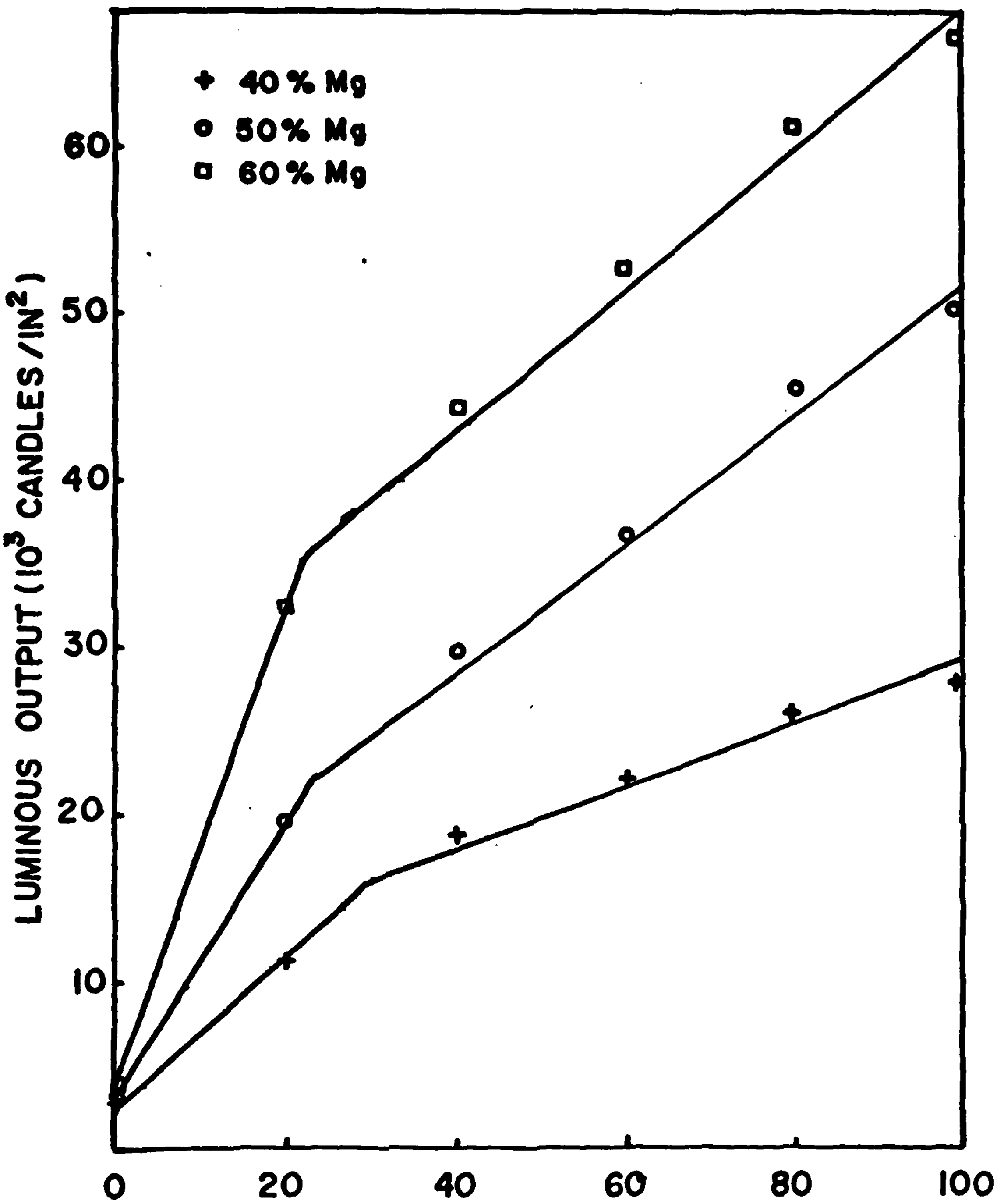

NOTE: Loading pressure = 10 kpsi

Figure 1. Effect of Mg and atmospheric O_2 content on luminous output

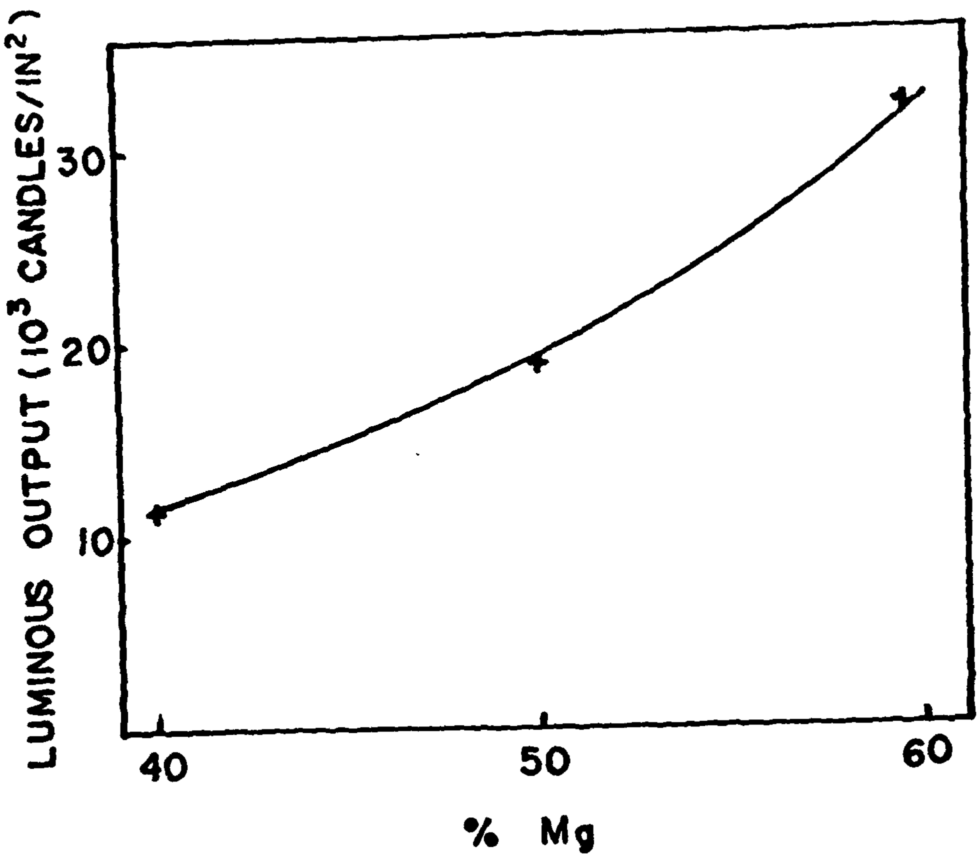

NOTE: Loading pressure = 10 kpsi

Figure 2. Effect of Mg content on luminous output of Mg-$NaNO_3$ compositions burning in 80% N_2/20% O_2 atmosphere

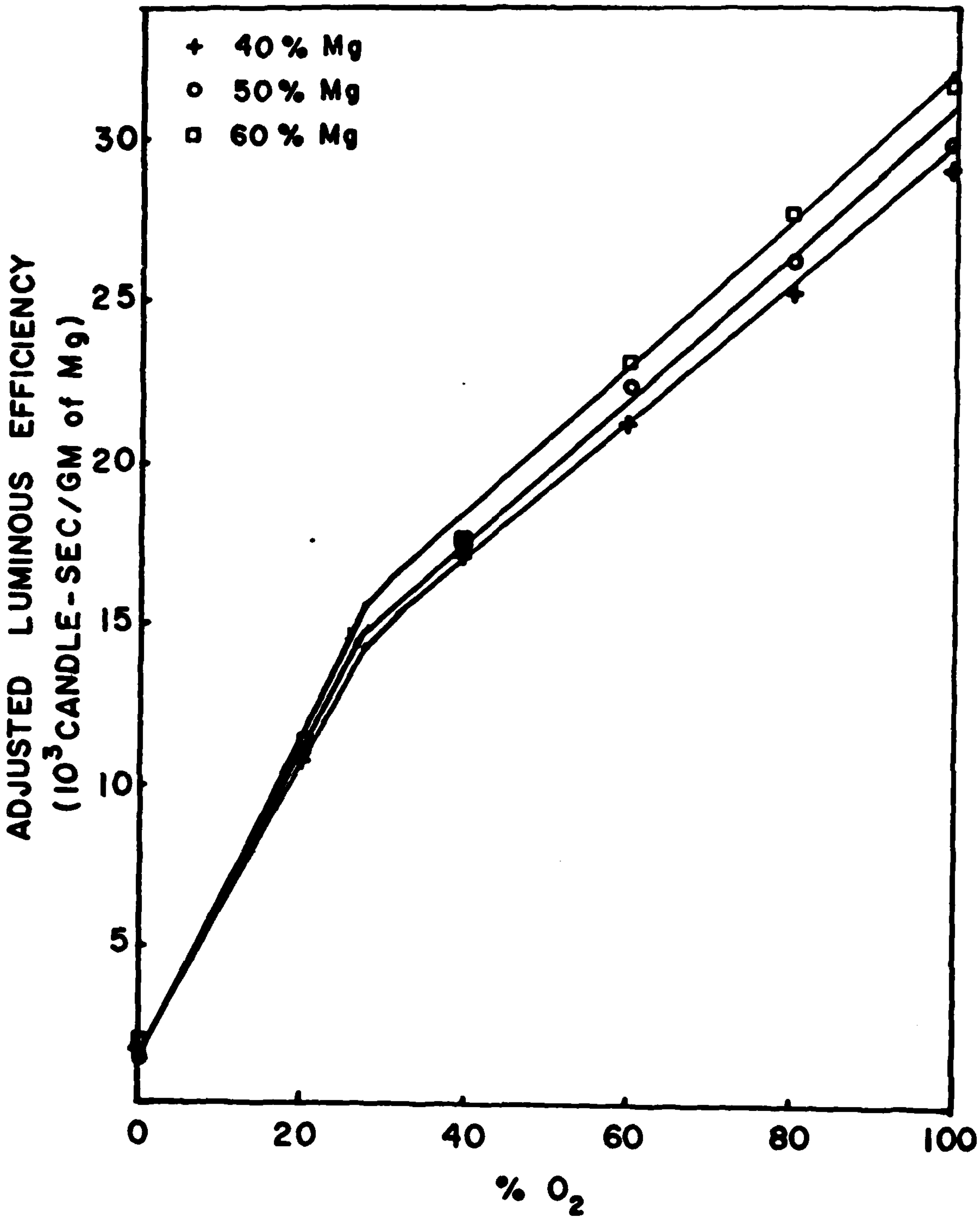

NOTE: Loading pressure = 10 kpsi

Figure 3. Effect of Mg and atmospheric O_2 contents on adjusted luminous efficiency

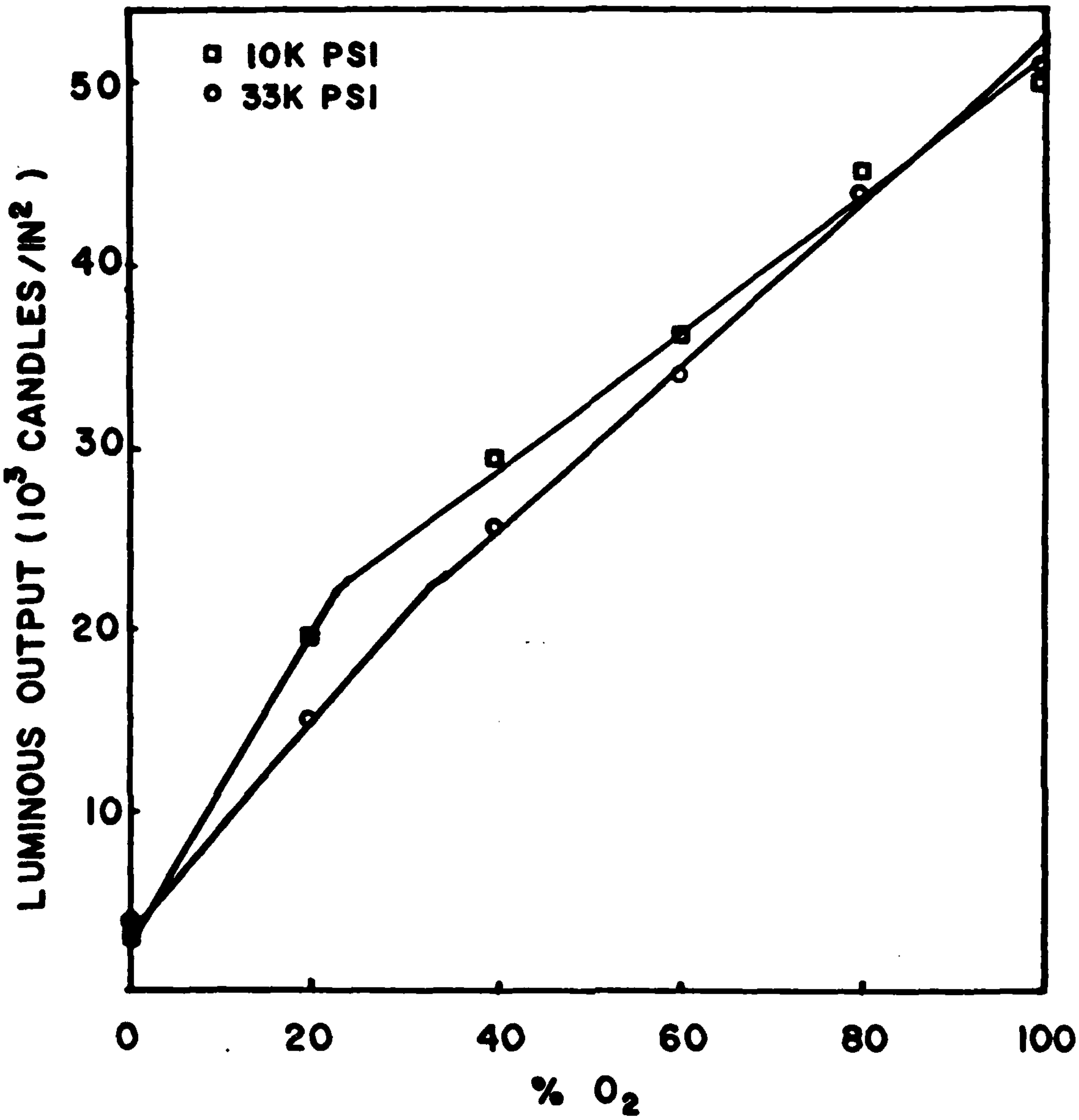

Figure 4. Effect of loading pressure and atmospheric O_2 content on luminous output of 50% Mg/50% $NaNO_3$ composition

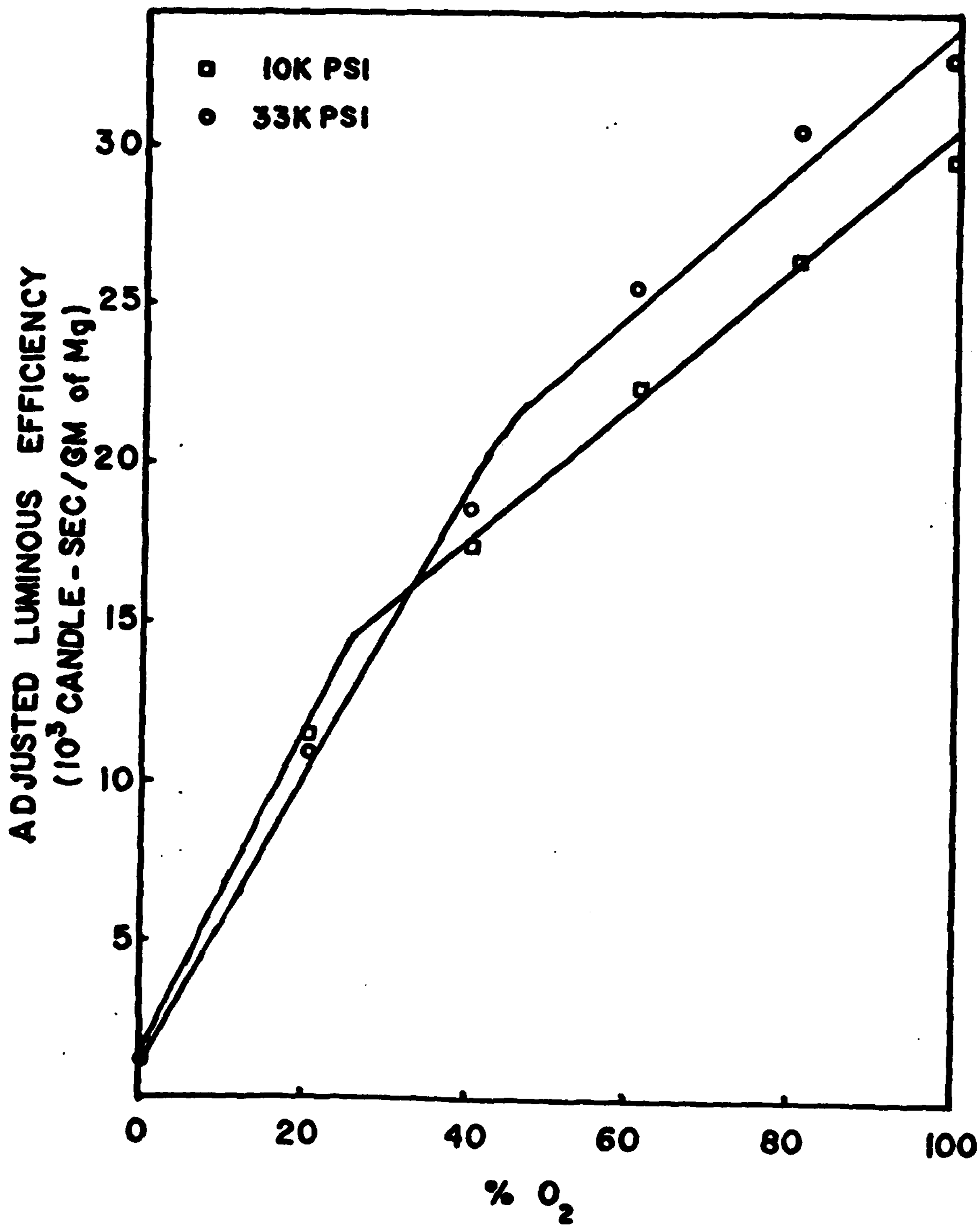

Figure 5. Effect of loading pressure and atmosphere O_2 content on adjusted luminous efficiency of 50% Mg/50% $NaNO_3$ composition

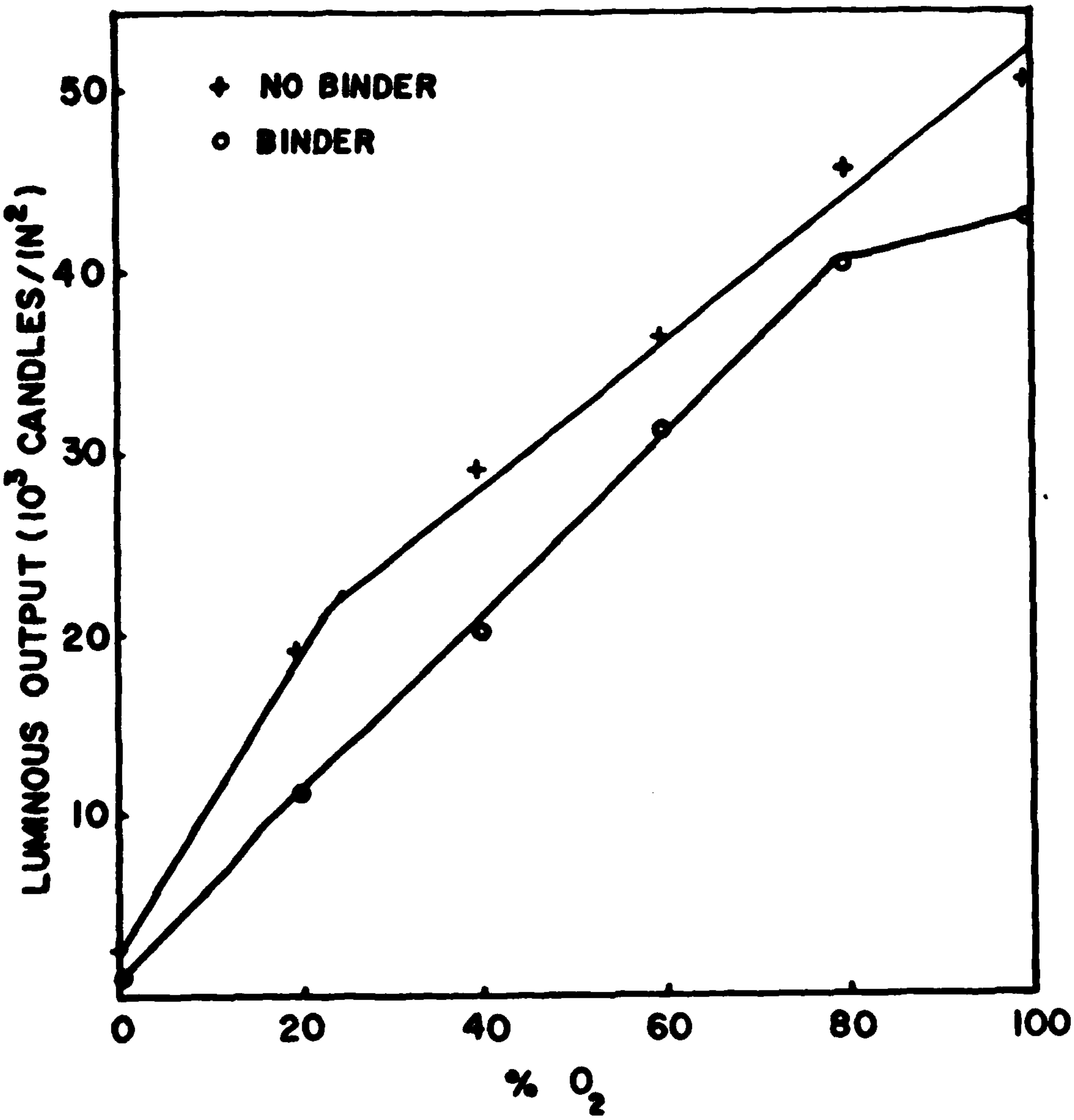

NOTE: Loading pressure = 10 kpsi

Figure 6. Effect of binder and atmosphere O_2 content on luminous output of 50% Mg/50% $NaNO_3$ composition

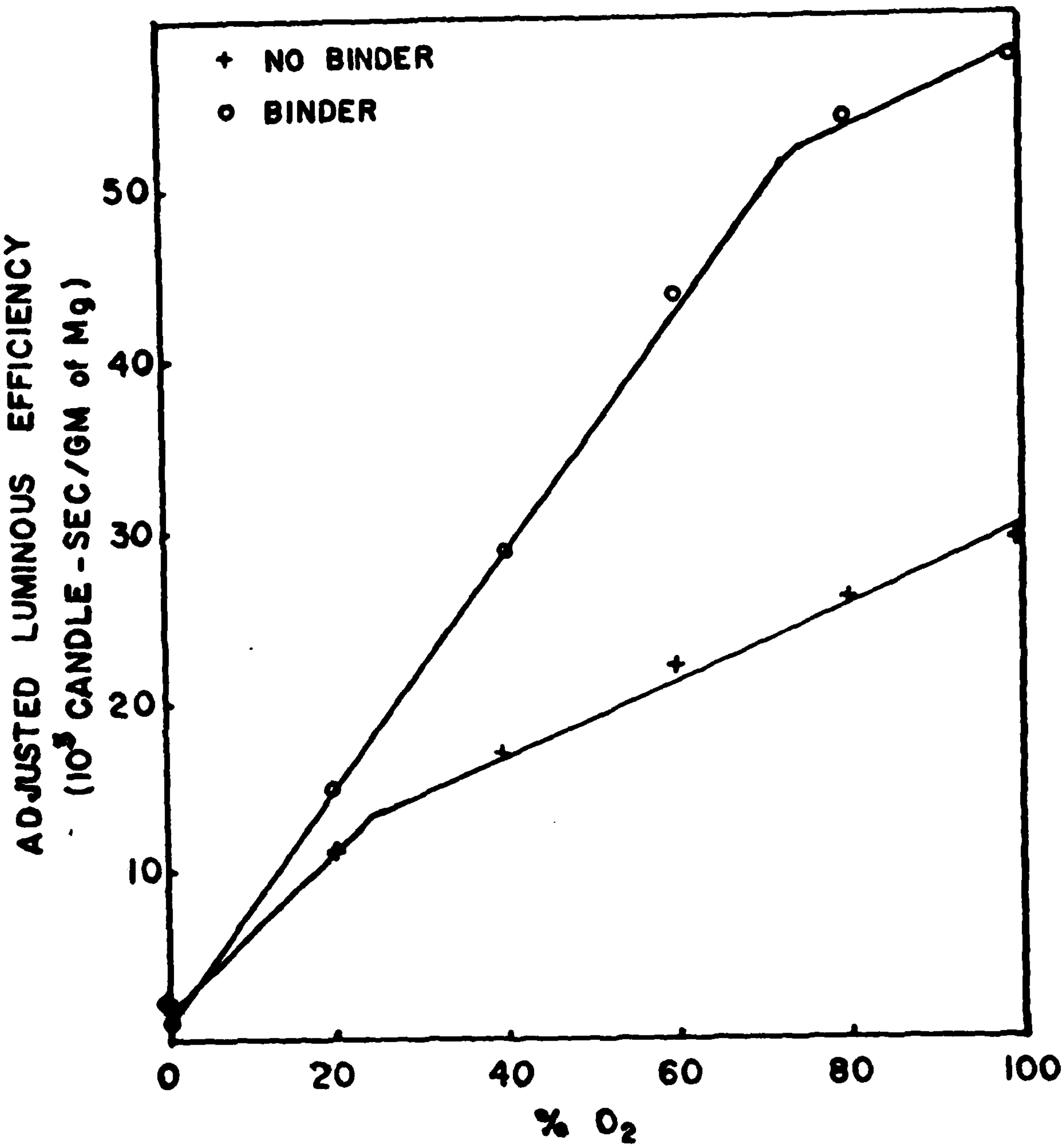

NOTE: Loading pressure = 10 kpsi

Figure 7. Effect of binder and atmospheric O_2 content on adjusted luminous efficiency of 50% Mg/50% $NaNO_3$ composition

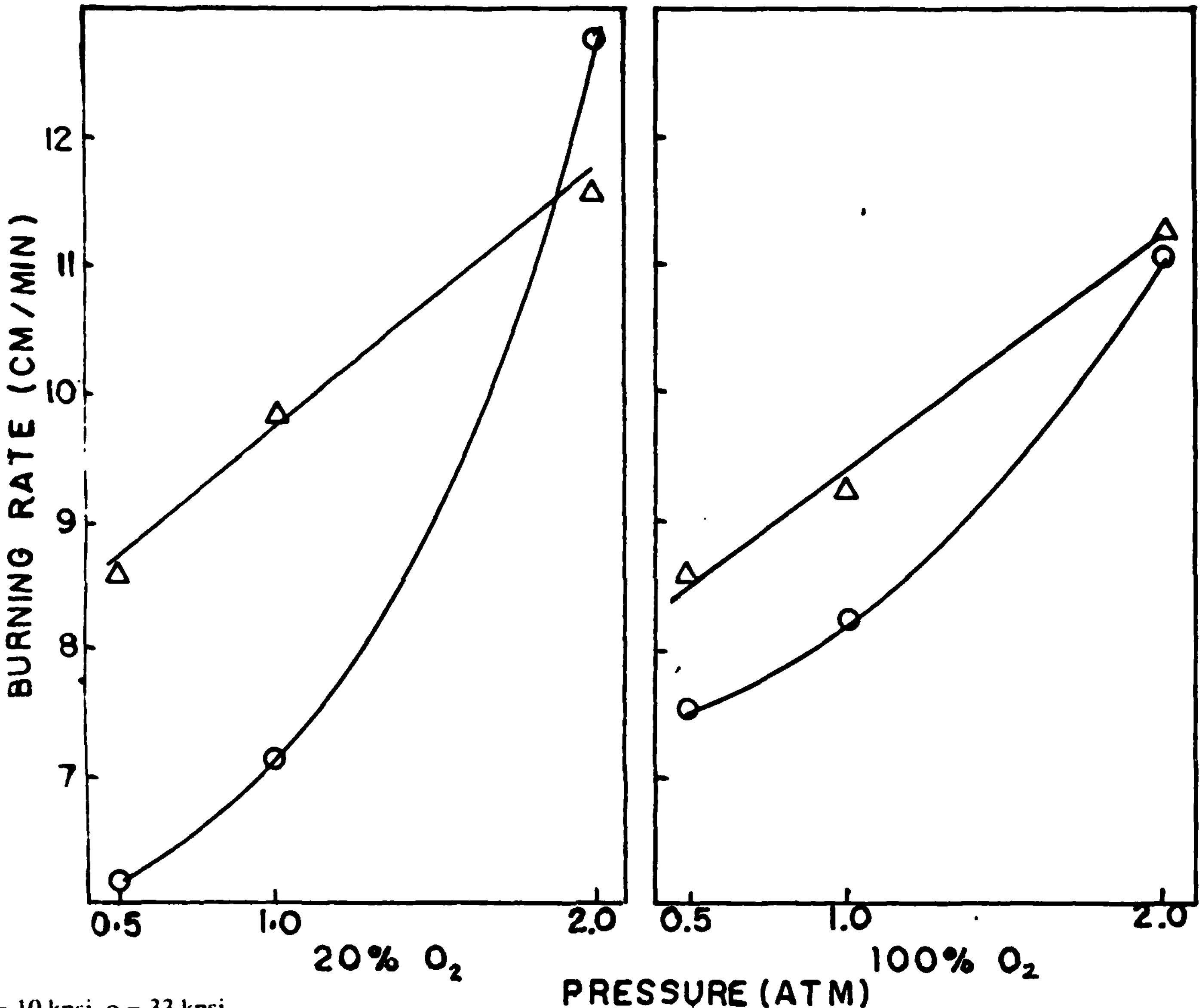

NOTE: Δ = 10 kpsi, o = 33 kpsi

Figure 8. Effects of atmospheric pressure on burning rate of Mg-$NaNO_3$ flares at several consolidation pressures

DISTRIBUTION LIST

Commander
Chemical Research, Development,
and Engineering Center
U.S. Army Armament, Munitions
Chemical Command
ATTN: SMCCR-MU, William Der
SMCCR-MUS-A, Joe Domanico
Aberdeen Proving Ground, MD 21010-5423

Director
U.S. Army Materiel Systems
Analysis Activity
ATTN: AMXSY-MP
Aberdeen Proving Ground, MD 21005-5066

Commander
Chemical Research, Development
and Engineering Center
U.S. Army Armament, Munitions
and Chemical Command
ATTN: SMCCR-MSI
Aberdeen Proving Ground, MD 21010-5423

Commander
Chemical Research, Development
and Engineering Center
U.S. Army Armament, Munitions
and Chemical Command
ATTN: SMCCR-RSP-A
Aberdeen Proving Ground, MD 21010-5423

Director
Ballistic Research Laboratory
ATTN: AMBXR-OD-ST
Aberdeen Proving Ground, MD 21005-5066

Commander
Armament Research, Development
 and Engineering Center
U.S. Army Armament, Munitions
 and Chemical Command
ATTN: SMCAR-IMI-I (5)
 SMCAR-AEE, Joseph Lannon
 SMCAR-AEE-P, Patricia Farnell (10)
 Francis R. Taylor
 L. Frey
Picatinny Arsenal, NJ 07806-5000

Commander
U.S. Army Armament, Munitions
 and Chemical Command
ATTN: AMSMC-GCL(D)
Picatinny Arsenal, NJ 07806-5000

Chief
Benet Weapons Laboratory, CCAC
Armament Research, Development
 and Engineering Center
U.S. Army Armament, Munitions
 amd Chemical Command
ATTN: SMCAR-CCB-TL
Watervliet, NY 12189-5000

Commander
U.S. Army Armament, Munitions
 and Chemical Command
ATTN: SMCAR-ESP-L
Rock Island, Il 61299-6000

Director
U.S. Army TRADOC Systems
 Analysis Activity
ATTN: ATAA-SL
White Sands Missile Range, NM 88002

U.S. Army Foreign Science and
 Technology Center
ATTN: Norm Taylor
Howard Sheinfeld
220 Seventh Street, NE
Charlottesville, VA 22901-5396

U.S. Army Research Office
ATTN: RDRD
P.O. Box 12211
Research Triangle Park, NC 27709

Naval Weapons Support Center
ATTN: Code 326, C.D. Robinson
Crane, IN 47522-5050

Commander
Naval Weapons Support Center
ATTN: Code 502, B. Douda
H. Webster
Crane, IN 47522-5050

Commander
Naval Weapons Center
ATTN: Code 3880, S. Reed
Code 233, Technical Library
China Lake, CA 93555-6001

Commander
Naval Surface Weapons Center
White Oak Laboratory
ATTN: Code X-21, Tech Library
Silver Springs, MD 20910

Commander
Naval Air Sytems Command
ATTN: Code AIR-954, Technical Library
Washington, DC 20361

Commander
Naval Sea Systems Command
ATTN: SEA-09G3, Technical Library
Washington, DC 20362-5101

Commander
U.S. Naval Ordnance Station
ATTN: Code 5124, Frank Valente
Scientific and Tech Info Div
Indian Head, MD 20640-5000

Commander
U.S. Air Force
ATTN: Library
Eglin Air Force Base, FL 32542

Aeronautical Systems Division (AFSC)
ATTN: Technical Library
Wright-Patterson Air Force Base
Ohio 45433

Commander
Air Force Avionics Laboratory (AFSC)
ATTN: AFAL/AAWW, F.D. Linton
Steve Wirick
Wright Patterson Air Force Base
Ohio 45433-6543

Commander
Harry Diamond Laboratories
ATTN: Library, Room 211, Bldg 92
Connecticut Avenue and Van Ness Street, NW
Washington, DC 20438

Defense Intelligence Agency
ATTN: DT-3B, William Lamb
Washington, DC 20301

Institute for Defense Analyses
ATTN: Library, Documents
400 Army-Navy Drive
Arlington, VA 22201

Administrator
Defense Technical Information Center
ATTN: Accessions Division (12)
Cameron Station
Alexandria, VA 22304-6145